OSCILLATION CONTROL OF A PENDULUM WITH SLIDING MASS AND PERTURBATION IN THE PIVOT

Mario Alberto Jordán[1] and José Luis Bonitatibus[1]

***Abstract*— We present a controller design based on parametric resonance concepts for a pendulum with erratic bounded motion of the support point and an actuator consisting of a sliding mass along the bar. The control algorithm is sustented on relations of potential/cinematic energy in synchronized manner according to principle of parametric resonance. In this way, the induced nonlinear oscillation of the pendulum is damped down using a generic control law. A bifurcation study is made for the Simulations and lab experiments with a prototype illustrate our approach.**

I. INTRODUCTION

In the framework of control of oscillations, physical pendulum has been investigated academically in many areas ranging from dynamics aspects, for instance in Control Theory ([8]; [2]; [13]) and nonlinear oscillations within the Theory of Bifurcations ([4]; [3]; [12]; [1]). There exists many applications where the system dynamics is partial or totally approximated by a pendulum-like dynamics, e.g., in buoys ([13]), cranes ([6]), manipulators ([9]), automatic balancer ([5]) among others.

The analysis of pendulum dynamics seems usually complex. Often the motion of pending loads excited through the pivot is handled as simple nonlinear pendulum. For small amplitudes one can apply the theory of Floquet for linear and periodic-varying dynamics ([7]). However the system contains nonlinearities that play an important role in the behavior and in the control of the induced nonlinear oscillations. The principles of control of pending weights, for instance in cranes, are based generally on horizontally or vertical displacement of the pivot with information of the pendulum angle and pivot position or cable length.

This paper explores the principle of parametric resonance and attempts to extend it to the control of nonlinear oscillations through a regulated time-varying mass center. To this end, the system is represented by a swinging bar subject to strong perturbations of the support point, while the actuator to exert the control action consists in a sliding mass along the bar (see Fig. 1). A controller for moving the sliding mass within a specified span is designed on the basis of a synchronism with the forced oscillation. So a significative nonlinear damping is created in the bar. A study of bifurcations in the controlled dynamics is carried out employing the frequency of the pivot motion in the main dimension and the span of the sliding mass position in the codimension. Alternatively, the midpoint of the oscillation is used as codimension in the analysis. Numerical simulations and runs in a prototype show the properties and advantages of the proposed oscillation control.

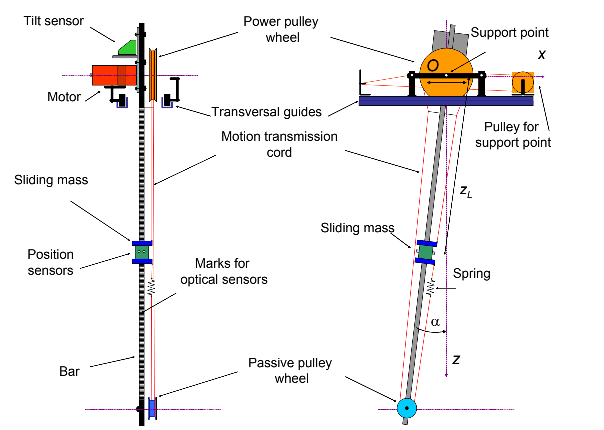

Sketch of a physical pendulum with moving mass and perturbed pivot

II. PENDULUM DYNAMICS

The pendulum dynamics in space state is deduced in the paper by stating the Lagrangian and Hamiltonian of the system. The resulting dynamics is

$$\ddot{\alpha} = -\frac{1}{I_0 + m\, z_L^2(t)}\left(\delta\, \dot{\alpha} + \frac{1}{2} g \sin\alpha\, \left(1 - \frac{d(t)}{L}\right) (L\, M_0 + 2\, m\, z_L(t)) + 2\, m\, \dot{\alpha}\, z_L(t)\, \dot{z}_L(t)\right), \quad (1)$$

where α is the bar angle, z_L the sliding mass position, d is the pivot displacement, I_0 is the bar inertia moment,

[1] Universidad Nacional del Sur, Argentine Institute of Oceanography (IADO-CONICET), Florida 8000, Complejo CRIBABB, Edificio E1, B8000FWB, Bahía Blanca, ARGENTINA. Corresponding Author: Mario A. Jordán: E-mail: mjordan@criba.edu.ar, Phone Tel: +54-291 4861309, Ext. 169, Fax: +54-291 486-1527/1112/1519

L the bar length, m the sliding mass, M_0 the bar mass, g the gravity acceleration, $\dot{\alpha}$ and $\dot{z}_L$ are rates of the oscillation and the slide velocity, respectively. For control purposes let us defined $u(t) = z_L(t)$ as the control action and $d(t)$ the pivot perturbation with

$$d(t) = L \, \varepsilon \sin(\omega t) \, , \tag{2}$$

and $0 \leq \varepsilon \leq 1$. Moreover, let us assume that $\dot{\alpha}$ and α are available for the control law while d is unknown and bounded.

III. Heuristics

The heuristics taken for controller design can be better illustrated with help of Fig. 2. Let us first consider null friction, the pivot fixed and an initial nonzero angle $\alpha(0)$. Assume the mass m is displaced between two levels in the bar according to the points 0 to 8 until completing a cycle and repeated again indefinitely. The time points to push down the mass are defined when $\dot{\alpha} = 0$, also the most slanted positions of the bar. Similarly, the time points to push up the mass occur when $\alpha = 0$, i.e., when the bar is on the vertical line. In completing this cycle, one can show in the paper that the maximal potential energy is reduced stepwise in each semi-cycle. So, with many successive cycles, the amplitude of the oscillation is reduced uniformly in time to null. On the other hand, if the cycles are made reversely, then the oscillation will be unstable.

A surprisingly feature of this synchronization is that the frequency of the mass is twice the frequency of the oscillation like in the parametric resonance property given by the Floquet theory for linear pendulum with harmonically moving pivot. Another property is that the enclosed areas in each cycle path are proportional to the lost mechanical energy per cycle.

IV. Control Algorithm

The proposed basic control law is a two-level algorithm and inspired in the heuristics developed previously. We suppose two specified mass levels termed z_{L_0} and z_{L_1} for the lower and upper levels in the bar, respectively, and a mass sliding velocity v. The synchronization of m according to the previous key idea occurs at points t_1 and t_2 in the mass descent from z_{L_1} to z_{L_0}, respectively, when the bar is more slanted. The mass ascent takes place at points t_3 and t_4 from z_{L_0} to z_{L_1}, respectively, with the bar crossing the vertical line. The mass will remain at z_{L_1} to z_{L_0}

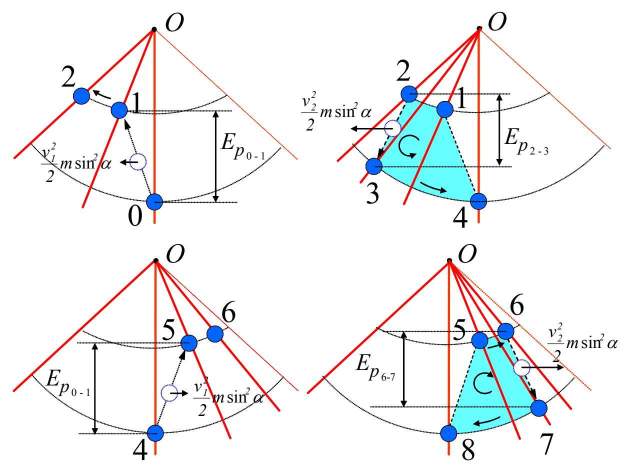

Fig. 1. Figure 2 - Cycle of the sliding mass for stable pendulum

as long as the synchronization conditions $\dot{\alpha}(t) = 0$ or $\alpha(t) = 0$ do not occur. Thus

$$\begin{cases} z_L(t) = z_{L_1} + \int_{t_1}^{t_2} v \; dt, \text{ from } t_1 \text{ up to } t_2, \\ \quad \text{where } t_1,\, t_2 \text{ fulfill: } \dot{\alpha}(t_1) = 0 \text{ and } z_L(t_2) = z_{L_0} \\ z_L(t) = z_{L_0} - \int_{t_3}^{t_4} v \; dt, \text{ from } t_3 \text{ up to } t_4, \\ \quad \text{where } t_3,\, t_4 \text{ fulfill: } \alpha(t_3) = 0 \text{ and } z_L(t_4) = z_{L_1} \\ z_L(t) = \text{constant from } t_2 \text{ to } t_3 \text{ and from } t_4 \text{ to } t_1 \,, \end{cases} \tag{3}$$

where the instants t_i will depend on the fulfillment of the synchronization conditions only.

There exists complex relations between the values of the set $\{z_{L_0}, z_{L_1}, \frac{z_{L_0}+z_{L_1}}{2}, v\}$ and the synchronism of the control system. Given a span and a midpoint there exists a critical sliding velocity to maintain the synchronism so that it is valid

$$t_2 - t_1 = \frac{z_{L_0} - z_{L_1}}{\bar{v}} \leq \frac{T_c}{4} \text{ and } t_4 - t_3 = \frac{z_{L_0} - z_{L_1}}{\bar{v}} \leq \frac{T_c}{4}, \tag{4}$$

where T_c is the period of the controlled oscillation of α and $\bar{v}$ the mean mass velocity which is considered equal in both ascent and descent.

There are many ways by which the basic control law can be optimized in the context of the control law (3). One important strategy is to accomplish a forced path of m such that the areas in each cycle be maximized. More precisely for a given pair of levels z_{L_0} and z_{L_1} the control law is optimized according to

$$\max_{\{t_1, t_3, z_{L_0}, z_{L_1}\}} \oint_{x\text{-}z} \operatorname{sign}(\alpha) \; A((z_L, v) \; ds \tag{5}$$

where the integral is the Green integral along the path $x(t)$-$z(t)$ and A is the area enclosed. Hence an optimal set $\{t_1, t_3, z_{L_0}, z_{L_1}\}$ is found according to the provided v and taking into account conditions (4).

V. Bifurcation analysis

In the rest of the paper we analyze the stability of the nonlinear oscillations for harmonic perturbations in the pivot. Both stationary and transient states are focused in the analysis. Basically we search the dynamics for large periods caused for a set of parameters characterized mainly for the excitation frequency with codimensions in the span and midpoint of the mass levels, and the sliding velocity of m.

The bifurcations diagrams are constructed as a series of power lines in the spectral function of the stationary orbit in the space $(\alpha, \dot{\alpha})$ for the basic control law. To this end, we employ the FFT function and classify the low-frequency power lines that are to the left of the excitation frequency. As a bifurcation occurs, a change in the periodicity or a chaotic behavior take place. These are detected by counting the number of low-frequency power lines plus one, which are plotted in the diagram for the main direction. Very high periods (i.e., higher than 10) or chaotic states are depicted by vertical segments.

Fig. 3 depicts the bifurcation diagram in form of power density functions of the first harmonic and subharmonics of the swing motion in the frequency domain for an uncontrolled pendulum (superior curve) and for four controlled pendulums with different mass ranges. Clearly, the uncontrolled pendulum behavior does not produce any bifurcation, yet the power of the oscillation for a fixed pivot frequency is almost greater tan the other cases, above all in low and mean frequencies. This is not the case with the controlled pendulums, whose behaviors show one periodic and high periodic oscillations, inclusive chaos, mainly for low frequencies and high frequencies. However, the power of this oscillation is drastically lower in these bands of the domain. Similar analysis and conclusions can be carried out from Fig. 4 when the mass velocity is put as codimension in the bifurcation diagram. However, if both results are compared, one can draw out that the mass velocity is much more effective to produce a strong nonlinear damping in the control behavior of the pendulum than the mass range.

In all cases, the power of the subharmonics is lower than that of the excitation frequency. On the other side, the superharmonics were not included in the diagram because they are relatively lower in power, inclusive in chaotic cases. Moreover, one knows that the fundamental frequency (referred here to as ω_0), it is, that one of the pivot excitation, corresponds to the largest power of the spectrum in all dimensions.

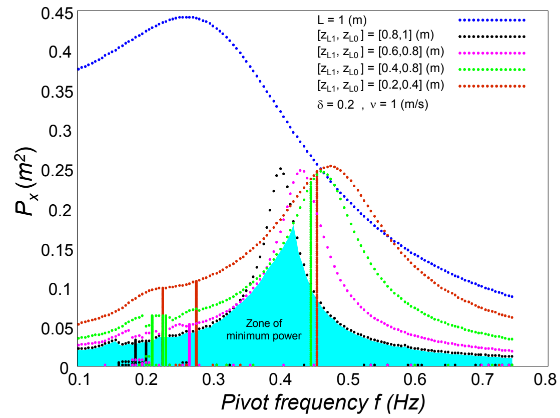

Figigure 3 - Zone of minimum energy according to bifurcation diagrams with variable range of mass displacement

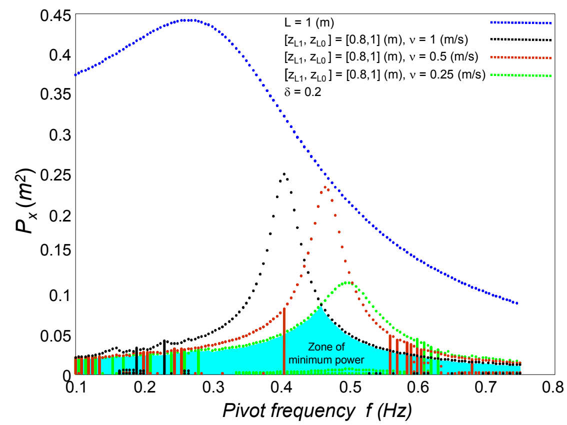

Figure 4 - Zone of minimum energy according to bifurcation diagrams with variable mass velocity

If now we interpolate the lower envelope of all bifurcation diagrams, we obtain a region of minimum energy. This is also illustrated in Figs. 3 and 4. As expected, the smallest zone corresponds to the codimension of the mass velocity and a mass range at the bottom extreme of the bar.

More surprisingly is that the envelope of this zone is composed by two bifurcation diagrams, namely those for extreme mass velocities. On the contrary, the envelope of the zone in Fig. 3 is composed by four stretches. For control purposes, the results in Fig. 4 seem to be more significative from the viewpoint of oscillation control than the results in Fig. 3.

The qualitative behavior of the system is good reflected in Poincaré maps in phase diagrams. In Fig. 5, for instance, the evolution of the control behavior for a chaotic case is illustrated.

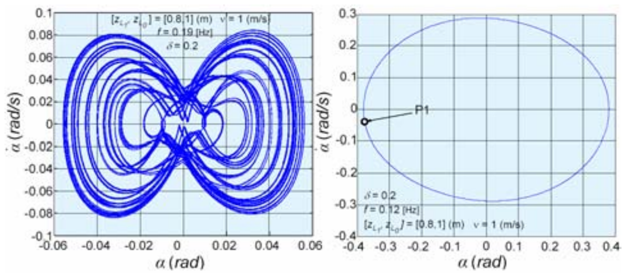

Figure 5 - Comparison of Poincaré maps between a chaotic orbit (strange attractor) and the uncontrolled orbit

Simultaneously, it is compared with the evolution of the pendulum without control. Clearly, the performance in steady state is quite superior in the control case from the viewpoint of the power attenuation. The change of the foregoing chaotic property to a lower periodic orbit can be appreciated in steady state in Fig. 6. This occurs when the frequency of excitation on the pivot changes slightly to 0.17 (Hz.). Doing it the periodicity becomes 3 in steady state. Also here, the power attenuation of the oscillation in comparison with the uncontrolled pendulum orbit is drastically reduced.

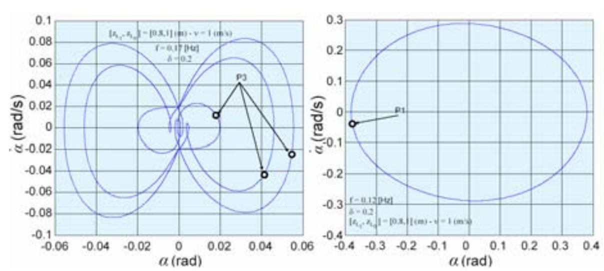

Figure 6 - Comparison of Poincaré maps between a periodic-3 orbit and the uncontrolled orbit

VI. Knowledge-based control algorithm

Based on previous results of the bifurcation analysis we propose now a knowledge-based algorithm that take advantage of the bifurcation diagrams in the main dimension and in the codimensions of mass rate and range. The key question is how this information is at the efficient as possible used on-line to rich the strongest nonlinear damping of the oscillations. First, we notice from previous Figs. 3 and 4 that the periodicity can be modified more easily by changing slightly the midpoint of the range of the sliding mass, *i.e.*, by adjusting the codimension of the mass range in the bifurcation diagram. However, the best way to maintain the energy of the orbit as low as possible is to regulate the mass rate (see Fig. 4). Hence, according to our expertise, we see the frequency $\omega_s = 0.47$ (Hz) as the critical frequency for switching properties of the control between the two tested velocities in our prototype.

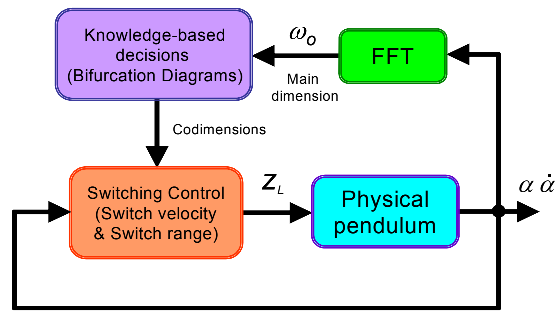

Figure 7 - Knowledge-based control diagram

One critical point in coordinating the switching of diagrams is to know the excitation frequency ω_0 of the pivot. To this end, we can sample continuously the orbit and analyze its power spectrum by means of an FFT algorithm. As we know, the maximal power line corresponds to the excitation, hence it is then easy to extract an estimation of ω_0.

The proposed algorithm is illustrated in Fig. 7. The basic switching control governs the sliding mass by achieving automatic synchronization with ω_0, but the optimal parameters to make orbits more predictable and/or with lowest energy are provided by employing knowledge of the codimensions in order to switch the best controller as in a gain-scheduling form.

It is worth noticing that the simplicity of the basic controller is maintained by the supervision loop. Basically the synchronization is not affected, only the range and rate of the sliding mass are modified in this framework as codimensions.

To illustrate the all-round evolution of the knowledge-based control system of Fig. 7, we propose an excitation $d(t)$ of 2 (m) of span and that can range within a wide interval of frequencies. The best way to see transitions of the dynamics is through an excitation $d(t)$ in form of chirp signal that changes its frequency linearly with time. In our study this frequency ω_0 increases from 0 up to 0.7 (Hz.) in 1000 (s) (see Fig 10a). The angle of the pendulum $\alpha(t)$ is represented in four cases according to: the uncontrolled case (Fig. 8b), the controlled case for minimal velocity v of m (see Fig. 8c), the controlled case for maximal velocity v of m (see Fig. 8d), and finally the proposed switching control (see Fig. 8e).

It is clearly seen that the switching control can obtained information on ω_0 via FFT on small periods of $\alpha(t)$ and detects the cross of the chirp signal by the critical frequency $\omega_s = 0.47$ (Hz) around 600 (s). Before this point is achieved, the algorithm detects lower frequencies and proposes the minimal velocity rate of the sliding mass. Then, after crossing ω_s, it determines the switching of the controller parameters automatically to the maximal velocity of m. The result is a drastic reduction of the energy of the oscillation. Clearly, the worst case corresponds to the uncontrolled pendulum.

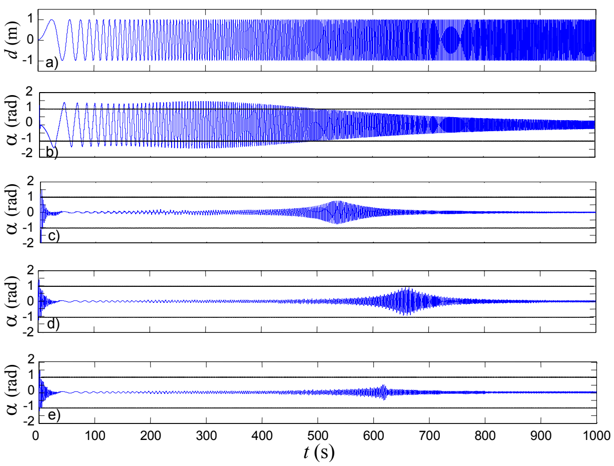

Figure 8 - a) Pivot motion in chirp form with f from 0 (Hz) up to 0.75 (Hz). b) without controller. c) Low-frequency controller. d) High-frequency controller. e) Knowledge-based switching controller.

VII. Conclusions

In this paper, a switching control system was designed for a perturbed physical pendulum. It is based on knowledge of qualitative and quantitative behavior in frequency domain. The controller criterion is supported by the synchronism between a sliding mass motion and the oscillation, like in the form of the parametric-resonance principle. The knowledge is sustained on the bifurcation diagrams in frequency domain as main dimension, and velocity of the sliding mass and its motion range as codimensions. The control algorithm identify the frequency of the excitation and detects a critical point to switch between optimal controllers according to the frequency. The achieved damping of this control system is notably larger as those obtained with other fixed controllers. This is illustrated in a case study. Future work concerns the completely implementation of the prototype depicted in Fig. 2.

References

[1] Leung, A.Y.T. and Kuang, J.L., "On the chaotic dynamics of a spherical pendulum with a harmonically vibrating suspension," *Nonlinear Dynamics*, Vol. 43 (3), 2006, pp 213-238.

[2] Abdel-Rahman, E.M. Nayfeh, A.H. and Masoud, Z.N., "Dynamics and control of cranes: A review," *Journal of Vibration and Control*, Vol. 9 (7), 2003, pp. 863-908.

[3] Ju, Y.S. Choo and F.S. Cui, "Dynamic response of tower crane induced by the pendulum motion of the payload," *International Journal of Solids and Structures*, Vol. 43 (2), 2006, pp. 376-389.

[4] Petrov, A.G., "On the equations of motion of a spherical pendulum with a fluctuating support," *Doklady Physics*, Vol. 50 (11), 2005, pp. 588-592.

[5] Horvath, R., Flowers, G.T. and Fausz, J., "Passive balancing for rotor systems using pendulum balancers," *Proceedings of the ASME International Design Engineering Technical Conferences and Computers and Information in Engineering Conference*, Vol. 1B, 2005, pp. 967-978.

[6] Kral, R., E. Kreuzer and C. Wilmers, Nonlinear oscillations of a crane ship, *Zeitschrift fur Angewandte Mathematik und Mechanik*, Vol. 76 (S4), 1996, pp. 5-8.

[7] Berkey, D.D., "An Asymptotic Floquet Theorem for Linear Almost Periodic Systems," *Siam J. Math. Anal.*, Vol. 7(6), 1976, pp. 843-847.

[8] Åström, K.J. and K. Furuta, Swinging-up a pendulum by energy control, In *Proceedings of the IFAC Congress*, Vol. E, 1996, pp. 37-42.

[9] Murat-Yeşiloğlu, S. and H. Temeltaş, "Balancing 3D objects with rolling constraint by redundant manipulator," *IEEE/ASME International Conference on Advanced Intelligent Mechatronics*, Vol. 2, 2005, pp. 1511-1516.

[10] Goldstein, H, "Classical Mechanics," *Addison Wesley*, 1980.

[11] Jordán M.A. and Bustamante, J.L., "Análisis de Oscilaciones No-lineales en Sistemas Complejos de Mecánica e Hidrodinámica - Herramientas y Metodología," *Revista Iberoamericana de Automática e Informática Industrial*, Vol. 1(3), pp. 68-77, 2004.

[12] Jordán, M.A., J.L. Bustamante, J.L., Bonitatibus, J.L. y Arlenghi, L.P., "Integración de Análisis Simbólico y Numérico en Sistemas Dinámicos Oscilantes de Ingeniería Oceánica," *V Simposio Argentino de Tecnología de la Comp.*, 20-24 Sept., 2004.

[13] Jordán, M.A., and J.L. Bonitatibus, "Parametric-Resonance-based Forced Dynamics for Wave-Excited Systems". *Reunión de Procesamiento de la Información y Control RPIC XI*, (CD-ROM), Río Cuarto, Argentina, Sept. 2005.